

Piezoelectric thin-film superlattices without using piezoelectric materials

N. D. Sharma,¹ C. M. Landis,³ and P. Sharma^{1,2,a)}

¹Department of Mechanical Engineering, University of Houston, Houston, Texas 77204, USA

²Department of Physics, University of Houston, Houston, Texas 77204, USA

³Aerospace Engineering and Engineering Mechanics, University of Texas at Austin, Texas 78712, USA

(Received 10 February 2010; accepted 10 April 2010; published online 20 July 2010)

In this paper we show that experimentally realizable *apparently piezoelectric thin-film superlattices* can be created from nonpiezoelectric materials provided an odd-order (e.g., trilayer) stacking sequence is used. The size-dependent mechanism of flexoelectricity, which couples gradients of strain to polarization, allows such a possibility. We present closed-form analytical expressions for the response of various thin-film and superlattice configurations. We also clarify some of the subtleties that arise in considering interface boundary conditions in the theory of flexoelectricity as well as the relationship of flexoelectricity to the frequently used polarization gradient terms used in modeling ferroelectrics. We find that for certain (optimum) material combinations and length scales, thin-film superlattices yielding apparent piezoelectricity close to 75% of ferroelectric barium titanate may be achievable. © 2010 American Institute of Physics. [doi:10.1063/1.3443404]

I. INTRODUCTION AND CENTRAL CONCEPT

In noncentrosymmetric dielectric crystals such as quartz and ZnO, a net electrical dipole moment is generated upon application of uniform strain due to relative displacements between the centers of oppositely charged ions. This well known phenomenon is known as piezoelectricity.^{1,2} Formally, the polarization vector is related to the second order strain tensor through the third order piezoelectric tensor as

$$P_i = p_{ijk}\epsilon_{jk}. \quad (1)$$

Being an odd-ordered tensor, p_{ijk} must vanish for all dielectrics with inversion-center symmetry, thus restricting existence of piezoelectricity to only noncentrosymmetric crystal structures. However, physically, this inversion symmetry of a dielectric unit cell can be broken locally by application of nonuniform strain or the presence of strain gradients. This contribution of macroscopic strain gradient toward induced polarization is known as the flexoelectric effect and can be written as

$$P_i = \underbrace{p_{ijk}\epsilon_{jk}}_{=0, \text{ for centrosymmetric materials}} + \mu_{ijkl} \frac{\partial \epsilon_{jk}}{\partial x_l}. \quad (2)$$

Here the fourth ordered tensor μ_{ijkl} is the so-called flexoelectric tensor, and is nonzero for crystals of any symmetry. This implies that under a nonuniform strain, all dielectric materials are capable of producing a polarization. Readers are referred to Ref. 3 and 4 for a review. The microscopic (atomic) underpinnings of flexoelectricity were recently discussed by one of us,⁵ where flexoelectric properties were atomistically calculated for several dielectrics of technological and scientific interest. An interesting example of the flexoelectric response is that of graphene (a manifestly nonpiezoelectric material) and clearly elucidated by the atomis-

tic calculations of Dumitrica *et al.*⁶ and Kalinin and Meunier.⁷

An estimate for lower bounds of the flexoelectric coefficients was provided by Kogan⁸ to be of the order of e/a ($\approx 10^{-9}$ C/m) which was corroborated for the case of an isotropic elastomer by Marvan *et al.*^{9,10} Here e is the electronic charge and a is lattice parameter. Later a simple linear chain model of ions¹¹ and experiments¹² suggested a dependence on the relative permittivity for the case of ordinary dielectrics. For ferroelectric perovskites like lead magnesium niobate (PMN), lead zirconate titanate (PZT), and barium strontium titanate (BST), even in the paraelectric phase, much larger magnitudes ($\approx 10^{-6}$ C/m) of flexoelectric coefficients than this lower bound are observed.¹³⁻¹⁸ Recently, Zubko *et al.*¹⁹ have published the experimental characterization of the complete flexoelectric tensor for SrTiO₃.

Several researchers have studied flexoelectricity recently and proposed various applications and consequences of this phenomenon. For example, Catalan *et al.*²⁰ have studied the impact of flexoelectricity on the dielectric properties and Curie temperature of ferroelectric materials while Cross and co-workers^{17,21} have proposed fabrication of piezoelectric composites without using piezoelectric materials. Eliseev *et al.*^{22,23} have investigated the renormalization in properties of ferroelectric nanostructures due to the spontaneous flexoelectric effect as well as analytical approaches to elucidate size-effects in such nanostructures.²⁴ In our previous work,²⁵ we computationally analyzed and demonstrated the possibility of designing such composites through suitable topology, constituent property differences, and the selection of optimum feature sizes. Such topologies are hard to realize in practice however. Nonpiezoelectric, tapered pyramidal structures on a substrate that “effectively” act as piezoelectric metamaterials have been fabricated in experimental studies by Cross,²⁶ Fu *et al.*,¹⁷ and Ma and Cross.¹⁶ A strong size-dependent enhancement of the apparent piezoelectric coefficient in materials that are intrinsically piezoelectric has been demonstrated by Majdoub *et al.*^{27,28} through atomistic calculations.

^{a)}Author to whom correspondence should be addressed. Electronic mail: psharma@uh.edu.

These flexoelectric composites have important technological ramifications such as in actuators, sensors, energy storage, and harvesting among others. In a recent work, Majdoub *et al.*²⁹ demonstrated, through first principles and theoretical calculations, that the so-called dead-layer effect in nanocapacitors may be strongly influenced by flexoelectricity. Several specialized topics have been well-reviewed in a recent book.³⁰

The central concept behind this paper (a continuation of our previous work,²⁵) is simple. Consider a composite consisting of two or more different nonpiezoelectric dielectric materials. Even under the application of uniform stress, differences in material properties at the interfaces will result in the presence of strain gradients. Those gradients will induce polarization due to the flexoelectric effect. For “properly designed” composites (clarified in Sec. III), the net average polarization will be nonzero. Thus, the nanostructure will exhibit an overall electromechanical coupling under uniform stress behaving like a piezoelectric material. The individual constituents must be at the nanoscale since this concept requires very large strain gradients and those (for a given strain) are generated easily only at the nanoscale.

While some general theoretical ideas behind the aforementioned concept were sketched out in a previous work,²⁵ the homogenization process was crude and the resulting three-dimensional topologies difficult to realize experimentally. In the present work we present closed-form solutions for easily-fabricated thin film superlattice structures that demonstrate the central concept in a transparent manner. The outline of the paper is as follows: In Sec. II, we review the basic theory of flexoelectricity, discuss some subtleties regarding the interfacial boundary conditions and comment on how flexoelectricity relates to the (often used) polarization gradient terms in modeling ferroelectrics. In Sec. III, we discuss the symmetry arguments that drive the creation of apparently piezoelectric superlattices without using piezoelectric materials. In Sec. IV, we provide general flexoelectricity solutions for the various thin-film layered configurations and calculate the overall electromechanical coupling.

II. THEORY OF FLEXOELECTRICITY, RELATION TO POLARIZATION GRADIENT THEORIES, AND INTERFACIAL BOUNDARY CONDITIONS

Within the assumptions of the linearized theory for *centrosymmetric* dielectrics, the Helmholtz energy density of deformation and polarization W^L can be assumed to be quadratic function of terms involving small strain e_{ij} , polarization P_i , polarization gradient $P_{i,j}$, and strain gradient $u_{j,kl}$ (Ref. 31)

$$\begin{aligned} W^L(P_i, e_{ij}, P_{i,j}, u_{j,kl}) = & \frac{1}{2} a_{kl} P_k P_l + \frac{1}{2} b_{ijkl} P_{i,j} P_{k,l} \\ & + \frac{1}{2} c_{ijkl} e_{ij} e_{kl} + d_{ijkl} P_{i,j} e_{kl} \\ & + f_{ijkl} P_i u_{j,kl}. \end{aligned} \quad (3)$$

Here, e_{ij} are the components of the strain tensor \mathbf{e} defined as

$$e_{ij} = \frac{1}{2} (u_{i,j} + u_{j,i}), \quad (4)$$

while $\mathbf{a}, \mathbf{b}, \mathbf{c}, \mathbf{d}, \mathbf{f}$ are material property tensors. In particular, “ \mathbf{a} ” and “ \mathbf{c} ” are the familiar second order reciprocal dielectric susceptibility and fourth order elastic constant tensors, respectively. The remaining tensors correspond to higher order electroelastic couplings which do not occur in the classical continuum description of an isotropic elastic dielectric. “ \mathbf{d} ,” which was introduced by Mindlin³² in his theory of polarization gradient, links gradients of polarization to strains while the components of “ \mathbf{f} ” are the flexoelectric coefficients.

If φ is the potential of the electric field \mathbf{E} given by

$$E_i = -\varphi_{,i}, \quad (5)$$

then the energy density of \mathbf{E} must be added to Eq. (4) yielding the total potential energy W

$$W = W^L + \frac{1}{2} \epsilon_0 \varphi_{,i} \varphi_{,j}. \quad (6)$$

Neglecting the effect of charge density as suggested by Askar *et al.*,³³ the total electric enthalpy density can be written as

$$\Sigma = W - (\epsilon_0 E_i + P_i) E_i, \quad (7)$$

which simplifies to

$$\begin{aligned} \Sigma = & \frac{1}{2} a_{kl} P_k P_l + \frac{1}{2} b_{ijkl} P_{i,j} P_{k,l} + \frac{1}{2} c_{ijkl} e_{ij} e_{kl} + d_{ijkl} P_{i,j} e_{kl} \\ & + f_{ijkl} P_i u_{j,kl} - \frac{1}{2} \epsilon_0 \varphi_{,i} \varphi_{,j} + P_i \varphi_{,i}. \end{aligned} \quad (8)$$

The tensor \mathbf{f} in Eq. (8) is related to the tensor $\boldsymbol{\mu}$ of Eq. (2) as⁵

$$f_{ijkl} = a_{im} (\mu_{mjkl} + \mu_{mjlk} - \mu_{mklj}). \quad (9)$$

All the tensors corresponding to the material properties are of even order since the restriction to centrosymmetry (i.e., classically nonpiezoelectric materials) requires that odd order tensors vanish.

The phenomenon of flexoelectricity in crystalline dielectrics was first predicted by Maskevich and Tolpygo³⁴ a phenomenological description was later proposed by Kogan⁸ who included a term coupling the polarization and the strain-gradient in the thermodynamic potential of the form

$$f_{ijkl} P_i u_{j,kl}. \quad (10)$$

Yet another body of work, which parallels the theory of flexoelectricity in some ways, is the polarization gradient theory due to Mindlin.^{35,36} Based on the long-wavelength limit of the shell-model of lattice dynamics, Mindlin³⁵ found that the core-shell and the shell-shell interactions could be incorporated phenomenologically by including the coupling of polarization gradients to strain and the coupling of polarization-gradients to polarization-gradients, respectively, in the thermodynamic potential [Eqs. (11a) and (11b)]

$$d_{ijkl} P_{i,j} e_{kl}, \quad (11a)$$

$$b_{ijkl}P_{i,j}P_{k,l}. \quad (11b)$$

Material property tensors \mathbf{d} and \mathbf{b} are constants introduced by Mindlin in this polarization gradient theory. The polarization-gradient strain coupling (represented by tensor \mathbf{d}) and the polarization strain-gradient coupling (represented by tensor \mathbf{f}) are often included in the energy density expression as a Lifshitz invariant³⁷ as shown in Eq. (12) on account of the fact that total derivatives cannot occur in the expression for energy,

$$h_{ijkl}(u_{i,j}P_{k,l} - P_{k,l}u_{i,j}). \quad (12)$$

This is justified if one considers the following argument. The contribution to the total energy of a finite volume of material including the flexoelectric and the polarization gradient term (only the one involving \mathbf{d}) is

$$\int_V (f_{ijkl}P_{i,j}u_{k,l} + d_{ijkl}P_{i,j}u_{k,l})dx. \quad (13)$$

Integration by parts yields:

$$\int_V (d_{ijkl}P_{i,j}u_{k,l} - f_{ijkl}P_{i,l}u_{j,k})dx + \text{Boundary terms}. \quad (14)$$

In other words, the governing equations remain unaltered if we use an expression of the form $(d_{ijkl}P_{i,j}u_{k,l} - f_{ijkl}P_{i,l}u_{j,k})$ as the energy density. Alternatively in terms of only one of the material tensors (say \mathbf{h}),

$$(d_{ijkl} - f_{iklj})P_{i,j}u_{k,l} = h_{ijkl}P_{i,j}u_{k,l}. \quad (15)$$

The contributions due to the term in the thermodynamic potential involving Mindlin's tensor \mathbf{d} and due to flexoelectricity (involving tensor \mathbf{f}) cannot be readily isolated from each other.⁵ Thus, mathematically, Mindlin's polarization gradient theory (1968) can be adapted to include the flexoelectric effect (strain gradient-polarization coupling) by replacing the coupling tensor \mathbf{d} by tensor \mathbf{h} as defined in Eq. (15). The new tensor \mathbf{h} thus derived represents combination of two fundamentally different coupling phenomena (i) strain-polarization gradient coupling (Mindlin's theory) and (ii) strain gradient-polarization coupling (flexoelectricity).

In order to further elucidate this assertion, we employ the following argument to recover expression (12). Consider

$$\int_V h_{ijkl}P_{i,j}u_{k,l}dx, \quad (16)$$

which can be decomposed as

$$\int_V \left(\frac{h_{ijkl}}{2}P_{i,j}u_{k,l} + \frac{h_{ijkl}}{2}P_{i,j}u_{k,l} \right) dx. \quad (17)$$

We employ integration by parts to yield

$$\int_V \left(\frac{h_{ijkl}}{2}P_{i,j}u_{k,l} - \frac{h_{ijkl}}{2}P_{i,l}u_{k,j} \right) dx + \text{Boundary terms}. \quad (18)$$

Thus an energy density of the following form can be recovered:

$$\frac{h_{ijkl}}{2}(P_{i,j}u_{k,l} - P_{i,l}u_{k,j}), \quad (19)$$

$\mathbf{h}/2$ can be redefined as \mathbf{g} to recover the form of expression (12). Thus, instead of introducing two separate tensors \mathbf{d} and \mathbf{f} , the enthalpy function can also be written as:²²

$$\begin{aligned} \Sigma = & \frac{1}{2}a_{kl}P_kP_l + \frac{1}{2}b_{ijkl}P_{i,j}P_{k,l} + \frac{1}{2}c_{ijkl}e_{ij}e_{kl} \\ & + \frac{1}{2}h_{ijkl}(P_{i,j}u_{k,l} - P_{k,l}u_{i,j}) - \frac{1}{2}\varepsilon_0\varphi_{,i}\varphi_{,j} + P_i\varphi_{,i}, \end{aligned} \quad (20)$$

where components of tensor \mathbf{h} are combination of components of tensor \mathbf{d} and tensor \mathbf{f} which occur in the energy density described by Eq. (8).

Standard variational analysis may now be employed to obtain a system of equilibrium equations, boundary conditions, and constitutive relations for an isotropic material occupying domain Ω and bounded by a surface S . We omit these details as such deductions are routine. The major variables, i.e., the electromechanical "stresses" are defined through the following relations:

$$\begin{aligned} \sigma_{ij} &\equiv \frac{\partial \Sigma}{\partial e_{ij}}, & t_{ijm} &\equiv \frac{\partial \Sigma}{\partial u_{i,jm}}, \\ \Lambda_{ij} &\equiv \frac{\partial \Sigma}{\partial P_{i,j}}, & \eta_i &\equiv \frac{\partial \Sigma}{\partial P_i}. \end{aligned} \quad (21)$$

The definition of σ_{ij} is the same as that of the stress tensor in classical elasticity; η_i is the effective local electric force. The terms t_{ijm} and Λ_{ij} can be thought of as higher order stresses (moment stress) and higher order local electric force, respectively. We now proceed to list the balance laws, boundary conditions and the constitutive relations.

(i) The balance laws.

$$(\sigma_{ij} - t_{ijm,m})_j + F_i = 0, \quad (22a)$$

$$\Lambda_{ij,j} + \eta_i - \phi_{,i} = 0 \quad (22b)$$

$$-\varepsilon_0\phi_{,ii} + P_{i,i} = 0 \quad \text{in } \Omega, \quad (22c)$$

$$\phi_{,ii} = 0 \quad \text{in } \Omega^*. \quad (22d)$$

In Eqs. (22a)–(22d), \mathbf{F} is external body force. In the absence of the higher order stress t_{ijm} which includes higher order gradients of the displacement vector (like $u_{i,jm}$), Eq. (22a) reduces to the standard force balance equation of classical elasticity.

Since the term $\sigma_{ij} - t_{ijm,m}$ occurs in a force balance relation as evident in Eq. (22a), we may interpret it as a "physical stress,"

$$\sigma_{ij}^{\text{phys}} = \sigma_{ij} - t_{ijm,m} \quad (23)$$

(ii) The boundary conditions.

For all $x \in S$, the following conditions hold:

$$n_i\sigma_{ij} = T_j, \quad (24a)$$

$$n_i\Lambda_{ij} = 0 \quad (24b)$$

$$n_i([\varepsilon_0\phi_{,i}] + P_i) = 0 \quad (24c)$$

$$[[P_i]] = 0 \quad (24d)$$

\mathbf{n} and \mathbf{T} are the exterior normal unit vector and the surface traction vector, respectively; ε_0 is the dielectric constant and the symbol $[[\]]$ denotes the jump across the surface S . Equation (24d), i.e., continuity of polarization, is an extra condition that must be imposed to obtain a closed set of equations.

(iii) The constitutive relations.

$$\sigma_{ij} = c_{ijkl}e_{kl} + d_{klij}P_{k,l}, \quad (25a)$$

$$t_{ijm,m} = f_{kijm}P_{k,m}, \quad (25b)$$

$$\Lambda_{ij} = b_{ijkl}P_{k,l} + d_{ijkl}e_{k,l}, \quad (25c)$$

$$-E_i = a_{ij}P_j + f_{ijkl}u_{j,k,l}. \quad (25d)$$

Substituting the constitutive relations (25a)–(25d) into the balance laws (22a)–(22d), yields the Navier-type equations for dielectrics that incorporate the strain-polarization gradient coupling (Mindlin's theory) and the strain gradient-polarization coupling (flexoelectricity)

$$c_{44}\nabla^2\mathbf{u} + (c_{12} + c_{44})\nabla\nabla\cdot\mathbf{u} + h_{12}\nabla^2\mathbf{P} + (h_{12} + h_{44})\nabla\nabla\cdot\mathbf{P} + \mathbf{F} = 0, \quad (26a)$$

$$h_{12}\nabla^2\mathbf{u} + (h_{12} + h_{44})\nabla\nabla\cdot\mathbf{u} + (b_{44} + b_{77})\nabla^2\mathbf{P} + (b_{12} + b_{44} - b_{77})\nabla\nabla\cdot\mathbf{P} - a\mathbf{P} - \nabla\phi + \mathbf{E}^0 = 0, \quad (26b)$$

$$-\varepsilon_0\nabla^2\phi + \nabla\cdot\mathbf{P} = 0. \quad (26c)$$

III. SINGLE THIN FILM AND SYMMETRY ARGUMENTS

Topologies of only certain symmetries can realize the central concept discussed in this paper. For example, isotropic spherical particles distributed in a matrix will not yield apparently piezoelectric composites even though the flexoelectric effect will cause local polarization fields. Due to spherical symmetry, the overall average polarization is zero. A similar composite but containing triangular shaped particles (and aligned in the same direction) will exhibit the required apparent piezoelectricity. Fabrication of the latter however is nontrivial.

In this section we explore symmetry considerations for the relatively easily manufacturable thin film based structures. Consider first a film made up of centrosymmetric material (Fig. 1). More complex thin-film configurations solutions can be built using the elementary solution to be presented.

For this film [idealized as a one-dimensional (1D) structure] the fields vary only in the x direction and the governing equations given by Eqs. (26a)–(26c) simplify to

$$c\frac{\partial^2 u}{\partial x^2} + (d-f)\frac{\partial^2 P}{\partial x^2} = 0,$$

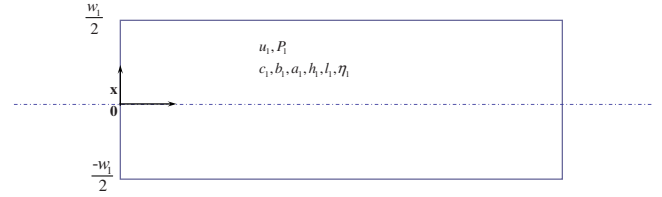


FIG. 1. (Color online) A thin film of a nonpiezoelectric material, e.g., paraelectric phase BaTiO₃.

$$(d-f)\frac{\partial^2 u}{\partial x^2} + b\frac{\partial^2 P}{\partial x^2} - aP - \frac{\partial\phi}{\partial x} = 0, \quad (27)$$

$$-\varepsilon_0\frac{\partial^2\phi}{\partial x^2} + \frac{\partial P}{\partial x} = 0.$$

Under open-circuit conditions, the electric displacement is zero

$$-\varepsilon_0\frac{\partial\phi}{\partial x} + P = 0. \quad (28)$$

We arrive at the following equations:

$$\frac{bc - (d-f)^2}{c}\frac{\partial^2 P}{\partial x^2} - (a + \varepsilon_0^{-1})P = 0, \quad (29a)$$

$$\Rightarrow \frac{\partial^2 P}{\partial x^2} - \frac{P}{l^2} = 0, \quad (29b)$$

where

$$l^2 = \frac{[bc - (d-f)^2]\varepsilon_0}{c\eta} \quad \text{and} \quad \eta = (1 + a\varepsilon_0). \quad (30)$$

Equation (30) can be solved for polarization to yield the form:

$$P = A_1 e^{(-x/l)} + A_2 e^{(x/l)}, \quad (31)$$

where A_1 and A_2 are the constants of integration. The displacement field is

$$u = A_3 + A_4 x + \frac{(d-f)}{c} e^{(-x/l)} (A_1 + A_2 e^{(2x/l)}). \quad (32)$$

Notice that in compliance with the Lifshitz invariance, the coefficients d and f appear together. For conciseness in the following sections, we write h instead of $(d-f)$.

We also define the stress and the electric tensors, respectively, as

$$\sigma = c\partial_x u + h\partial_x P, \quad (33a)$$

$$\Lambda^{(ij)} = h\partial_x u + b\partial_x P. \quad (33b)$$

For the thin-film in Fig. 1, the following boundary conditions must be satisfied.

1. Applied stress boundary conditions

$$(c_1\partial_x u_1 + h_1\partial_x P_1) = \sigma. \quad (34)$$

2. Electric tensor is set to zero at the free boundaries

$$(h_1\partial_x u_1 + b_1\partial_x P_1)|_{x \rightarrow \pm \frac{w_1}{2}} = 0, \quad (35a)$$

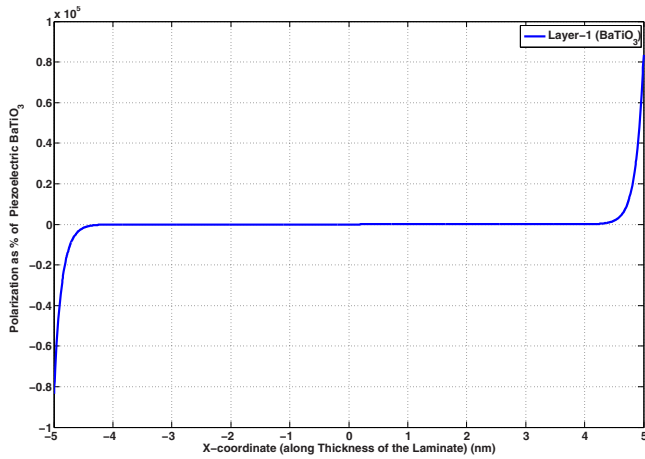


FIG. 2. (Color online) Polarization distribution in a thin film of paraelectric BaTiO₃. Total average polarization in the film is zero.

$$(h_1 \partial_x u_1 + b_1 \partial_x P_1)|_{x \rightarrow -w_1/2} = 0. \quad (35b)$$

3. Displacement u is set to zero at the origin

$$(u_1)|_{x \rightarrow 0} = 0. \quad (36)$$

Solving Eqs. (34), (35a), (35b), and (36) along with Eqs. (31), (32), (33a), and (33b), we obtain the expressions for polarization and displacement as

$$P_1 = - \frac{\sigma \operatorname{sech}\left(\frac{w_1}{2l_1}\right) \sinh\left(\frac{x_1}{l_1}\right) h_1 \varepsilon_0}{c_1 l_1 \eta_1}, \quad (37a)$$

$$u_1 = \frac{\sigma}{c_1} \left(x + \frac{\sigma \operatorname{sech}\left(\frac{w_1}{2l_1}\right) \sinh\left(\frac{x_1}{l_1}\right) h_1^2 \varepsilon_0}{c_1 l_1 \eta_1} \right). \quad (37b)$$

The average polarization, as evident, is zero,

$$\frac{1}{w_1} \int_{-w_1/2}^{w_1/2} P_1 dx = 0. \quad (38)$$

To provide some physical perspective, we plot the polarization field for a 10 nm paraelectric BaTiO₃ (Fig. 2). The applied stress is unity and the material constants are presented in table in Appendix.

Building on the general solutions for the 1D monolayer structure derived here, we can analyze various superlattices for the induced average polarization. Explicit expressions for induced polarization in each layer of the superlattice can be derived and used to calculate the averaged polarization in the entire composite.

A single thin film discussed so far is centrosymmetric about the mid-line. While a *finite* bilayer is noncentrosymmetric, a periodic two layered superlattice (a sequence of A-B-A-B-A-B...) is centrosymmetric. However, a trilayer sequence, e.g., A-B-C-A-B-C is noncentrosymmetric. In general, any odd-order stacking (of which A-B-C stacking is the simplest example) should yield a net nonzero average polarization.

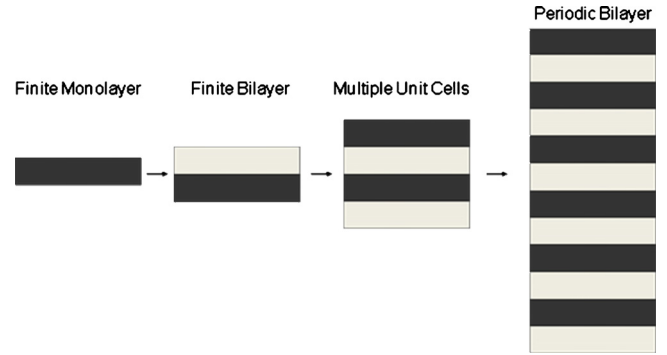


FIG. 3. (Color online) Apparently piezoelectric monolayer, finite bilayer, and periodic bilayer. In case of periodic bilayer, the average polarization is zero.

Consider a periodic bilayer as shown in Fig. 3. Each layer of a periodic bilayer experiences the strain gradients of same magnitudes in opposite directions at each interface. As a result of this “inversion symmetry” of strain gradient the dipole moment induced in one layer of a unit cell is negated by the dipole moment induced in the next layer, rendering the overall average polarization in the composite to be zero. In other words the induced dipole moment in a layer negates the dipole moment induced in the adjacent layer. Thus overall average polarization in a periodic two layered superlattice is zero.

We must break this symmetry in order to get an apparent piezoelectric behavior in the periodic superlattices. The careful choice of material properties and superlattice topology can break the geometric centrosymmetry. If one introduces a third layer as shown in Fig. 4(b), the inversion symmetry is broken in such a periodic system. This periodic trilayered superlattice thus is capable of generating a nonzero averaged polarization in the system.

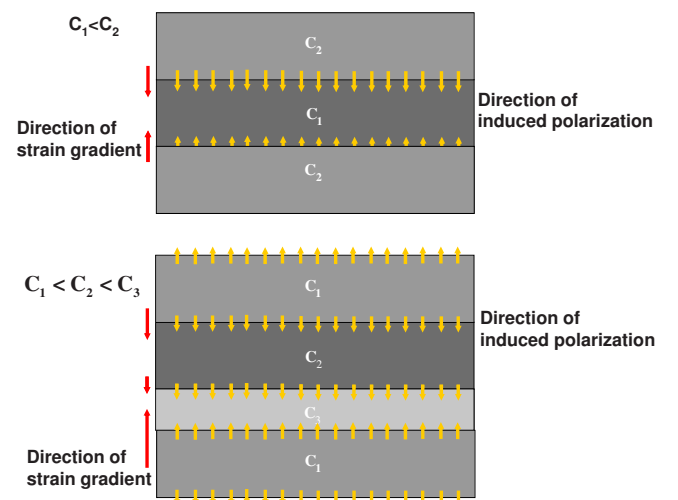


FIG. 4. (Color online) (a) Schematic of a periodic bilayer superlattice where induced dipole moment in a layer negates the dipole moment induced in the adjacent layer. Thus overall average polarization in a periodic bilayer superlattice is zero. (b) Schematic of a periodic trilayer superlattice shows that careful choice of material properties and superlattice topology can break the geometric centrosymmetry. Averaged strain gradients and thus the averaged induced polarization over the unit cell of a periodic trilayer superlattice are nonzero.

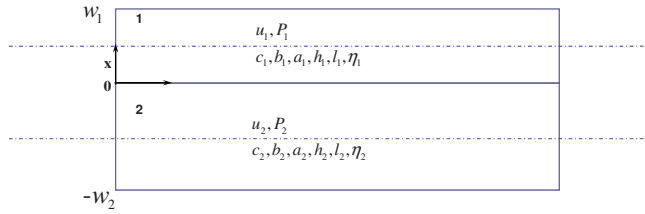


FIG. 5. (Color online) Unit cell of a bilayer film.

IV. MULTILAYER THIN FILMS AND SUPERLATTICES

In an attempt to break the inherent centrosymmetry associated with a single thin film, we first consider a finite (nonperiodic) bilayer with thicknesses w_1 and w_2 as shown in the Fig. 5.

Even under application of uniform stress, change in material properties at the interface of the two layers will result in the presence of strain gradients in the system, which will induce polarization due to the flexoelectric coupling. Note that in the finite case, such structures will in fact lack the inversion symmetry of individual layers around the interface of the two layers. Thus, we would expect a nonzero average polarization under suitable boundary conditions. As derived in Sec. III, the polarization and displacement in layer-1 is of the form

$$P_1 = A_{11} \exp\left(-\frac{x}{l_1}\right) + A_{12} \exp\left(\frac{x}{l_1}\right), \quad (39a)$$

$$u_1 = A_{13} + A_{14}x + \frac{h_1}{c_1} \exp\left(-\frac{x}{l_1}\right) \left[A_{11} + A_{12} \exp\left(2\frac{x}{l_1}\right) \right]. \quad (39b)$$

Similarly, in layer-2, the polarization and displacement is given by

$$P_2 = A_{21} \exp\left(-\frac{x}{l_2}\right) + A_{22} \exp\left(\frac{x}{l_2}\right), \quad (40a)$$

$$u_2 = A_{23} + A_{24}x + \frac{h_2}{c_2} \exp\left(-\frac{x}{l_2}\right) \left[A_{21} + A_{22} \exp\left(2\frac{x}{l_2}\right) \right]. \quad (40b)$$

The following boundary conditions must be satisfied.

1. Applied stress boundary conditions

$$(c_1 \partial_x u_1 + h_1 \partial_x P_1) = \sigma, \quad (41a)$$

$$(c_2 \partial_x u_2 + h_2 \partial_x P_2) = \sigma. \quad (41b)$$

2. Continuity of stress at the interface

$$[[\sigma]]_{x \rightarrow 0} = (\sigma^{(1)})_{x \rightarrow 0} - (\sigma^{(2)})_{x \rightarrow 0} = 0. \quad (42)$$

This condition is redundant, since in this case, the previous two (applied stress) conditions trivially ensure this continuity.

3. Displacements at the interface are zero

$$u_1|_{x \rightarrow 0} = 0, \quad (43a)$$

$$u_2|_{x \rightarrow 0} = 0. \quad (43b)$$

4. Electric tensor E_{ij} is set to zero at the free boundaries

$$\Lambda_{ij}^{(1)} = (h_1 \partial_x u_1 + b_1 \partial_x P_1)|_{x \rightarrow w_1} = 0, \quad (44a)$$

$$\Lambda_{ij}^{(2)} = (h_2 \partial_x u_2 + b_2 \partial_x P_2)|_{x \rightarrow -w_2} = 0. \quad (44b)$$

5. The Electric tensor (E_{ij}) is specified to be continuous (but not necessarily zero) at the interface

$$[[\Lambda_{ij}]]_{x \rightarrow 0} = (\Lambda_{ij}^{(1)})_{x \rightarrow 0} - (\Lambda_{ij}^{(2)})_{x \rightarrow 0} = 0. \quad (45)$$

6. Polarization (P) is specified to be continuous at the interface

$$[[P]]_{x \rightarrow 0} = (P_1)_{x \rightarrow 0} - (P_2)_{x \rightarrow 0} = 0. \quad (46)$$

Unlike classical theory of piezoelectricity, an additional boundary condition is required at the interface on the polarization field.

We finally obtain the following results:

$$P_1 = - \frac{\sigma \epsilon_0 \left(-\cosh\left(\frac{x-w_1}{l_1}\right) \left[-1 + \cosh\left(\frac{w_2}{l_2}\right) \right] c_1 h_2 l_1 \eta_1 + c_2 h_1 \left\{ \left[-\cosh\left(\frac{x}{l_1}\right) + \cosh\left(\frac{x-w_1}{l_1}\right) \right] \cosh\left(\frac{w_2}{l_2}\right) l_1 \eta_1 - \sinh\left(\frac{x}{l_1}\right) \sinh\left(\frac{w_2}{l_2}\right) l_2 \eta_2 \right\} \right)}{c_1 c_2 l_1 \eta_1 \left[\cosh\left(\frac{w_2}{l_2}\right) \sinh\left(\frac{w_1}{l_1}\right) l_1 \eta_1 + \cosh\left(\frac{w_1}{l_1}\right) \sinh\left(\frac{w_2}{l_2}\right) l_2 \eta_2 \right]} \quad (47)$$

and

$$P_2 = \frac{\sigma \epsilon_0 \left(\left[-1 + \cosh\left(\frac{w_1}{l_1}\right) \right] \cosh\left(\frac{x+w_2}{l_2}\right) c_2 h_1 l_2 \eta_2 + c_1 h_2 \left\{ -\sinh\left(\frac{w_1}{l_1}\right) \sinh\left(\frac{x}{l_2}\right) l_1 \eta_1 + \cosh\left(\frac{w_1}{l_1}\right) \left[\cosh\left(\frac{x}{l_2}\right) - \cosh\left(\frac{x+w_2}{l_2}\right) \right] l_2 \eta_2 \right\} \right)}{c_1 c_2 l_2 \eta_2 \left[\cosh\left(\frac{w_2}{l_2}\right) \sinh\left(\frac{w_1}{l_1}\right) l_1 \eta_1 + \cosh\left(\frac{w_1}{l_1}\right) \sinh\left(\frac{w_2}{l_2}\right) l_2 \eta_2 \right]}. \quad (48)$$

Average polarization in the superlattice is calculated to be

$$\frac{1}{w_1 + w_2} \left(\int_0^{w_1} P_1 dx + \int_{-w_2}^0 P_2 dx \right) = \frac{4\sigma \sinh\left(\frac{w_1}{2l_1}\right) \sinh\left(\frac{w_2}{2l_2}\right) \epsilon_0 (\eta_1 - \eta_2) \left[\cosh\left(\frac{w_1}{2l_1}\right) \sinh\left(\frac{w_2}{2l_2}\right) c_1 h_2 l_1 \eta_1 + \cosh\left(\frac{w_2}{2l_2}\right) \sinh\left(\frac{w_1}{2l_1}\right) c_2 h_1 l_2 \eta_2 \right]}{c_1 c_2 (w_1 + w_2) \eta_1 \eta_2 \left[\cosh\left(\frac{w_2}{l_2}\right) \sinh\left(\frac{w_1}{l_1}\right) l_1 \eta_1 + \cosh\left(\frac{w_1}{l_1}\right) \sinh\left(\frac{w_2}{l_2}\right) l_2 \eta_2 \right]} \quad (49)$$

We note here that the average polarization directly depends on the difference between the dielectric constants of the constituent materials. Larger differences between the dielectric constants of the two layers leads to a larger induced average polarization, which translates into a stronger apparent piezoelectric behavior. Numerical results for BaTiO₃–MgO bilayer are shown in Fig. 6. For these results, we assume both layers, layer-2 (MgO) and layer-1 (BaTiO₃) to be 10 nm thick subject to a unit applied stress.

In the case of a finite two layered film structure made up of nonpiezoelectric materials the averaged net polarization is nonzero and for the numerical results shown in Fig. 6, we obtain an effective piezoelectric constant of about 23% of BaTiO₃—a well known piezoelectric material.

A. Periodic two layered superlattices

Consider a *periodic* bilayer superlattice (A-B-A-B sequence). In addition to the boundary conditions presented earlier, we impose periodicity requirement

$$P_1|_{x \rightarrow w_1} = P_2|_{x \rightarrow -w_2}, \quad (50a)$$

$$E_{ij}^{(1)}|_{x \rightarrow w_1} = E_{ij}^{(2)}|_{x \rightarrow -w_2}. \quad (50b)$$

The final results are

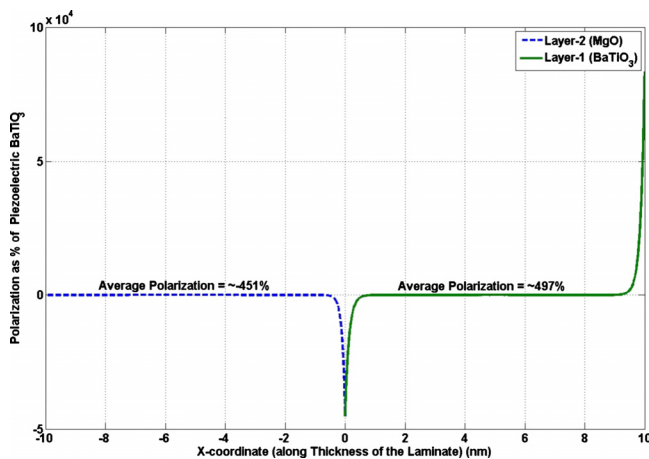


FIG. 6. (Color online) Polarization distribution in each layer of a MgO–BaTiO₃ finite bilayer. Total average polarization in the bilayer is 23% of piezoelectric BaTiO₃.

$$P_1 = \frac{\sigma \sinh\left(\frac{-2x + w_1}{2l_1}\right) \sinh\left(\frac{w_2}{2l_2}\right) (c_2 h_1 - c_1 h_2) \epsilon_0}{c_1 c_2 \left[\cosh\left(\frac{w_1}{2l_1}\right) \sinh\left(\frac{w_2}{2l_2}\right) l_1 \eta_1 + \cosh\left(\frac{w_2}{2l_2}\right) \sinh\left(\frac{w_1}{2l_1}\right) l_2 \eta_2 \right]} \quad (51)$$

and

$$P_2 = \frac{\sigma \sinh\left(\frac{w_1}{2l_1}\right) \sinh\left(\frac{2x + w_2}{2l_2}\right) (c_2 h_1 - c_1 h_2) \epsilon_0}{c_1 c_2 \left[\cosh\left(\frac{w_1}{2l_1}\right) \sinh\left(\frac{w_2}{2l_2}\right) l_1 \eta_1 + \cosh\left(\frac{w_2}{2l_2}\right) \sinh\left(\frac{w_1}{2l_1}\right) l_2 \eta_2 \right]} \quad (52)$$

As expected from symmetry arguments, the overall average polarization is zero (see Fig. 7)

$$\frac{1}{w_1 + w_2} \left(\int_0^{w_1} P_1 dx + \int_{-w_2}^0 P_2 dx \right) = 0. \quad (53)$$

B. Periodic trilayer

Consider a periodic trilayer as shown in the Fig. 8.

Note that the origin is defined at interface of layer-2 and layer-3. The general forms of the polarization and displacement fields are

$$P_1 = A_{11} \exp\left(-\frac{x}{l_1}\right) + A_{12} \exp\left(\frac{x}{l_1}\right), \quad (54a)$$

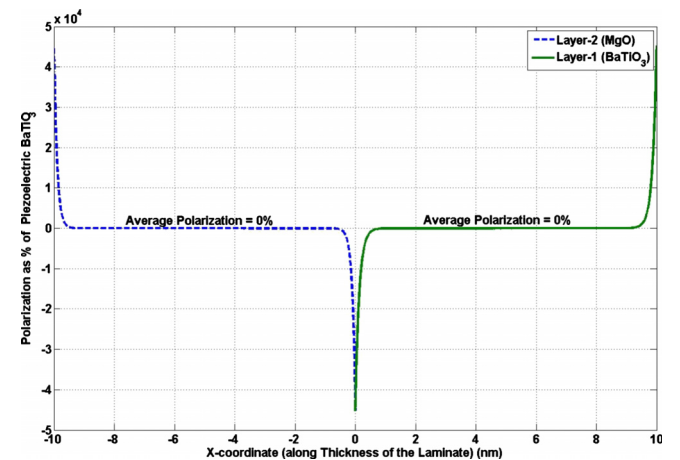


FIG. 7. (Color online) Polarization in each layer of a MgO–BaTiO₃ Periodic two layered superlattice.

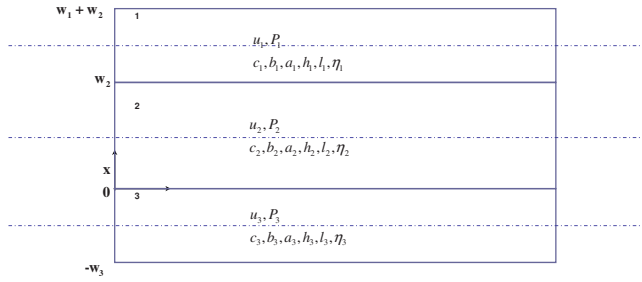


FIG. 8. (Color online) Unit cell of a three layered superlattice.

$$u_1 = A_{13} + A_{14}x + \frac{h_1}{c_1} \exp\left(-\frac{x}{l_1}\right) \left[A_{11} + A_{12} \exp\left(2\frac{x}{l_1}\right) \right], \quad (54b)$$

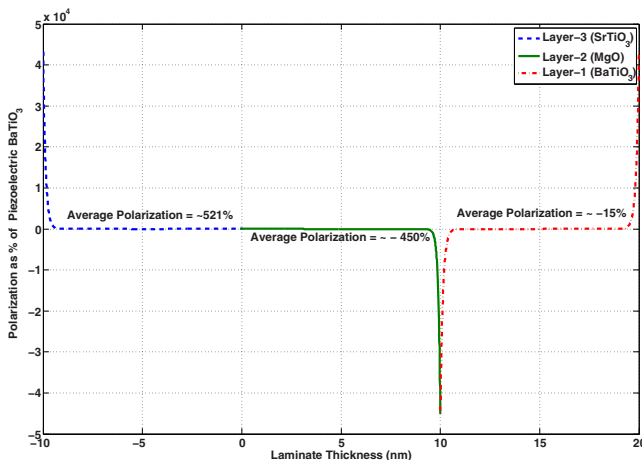
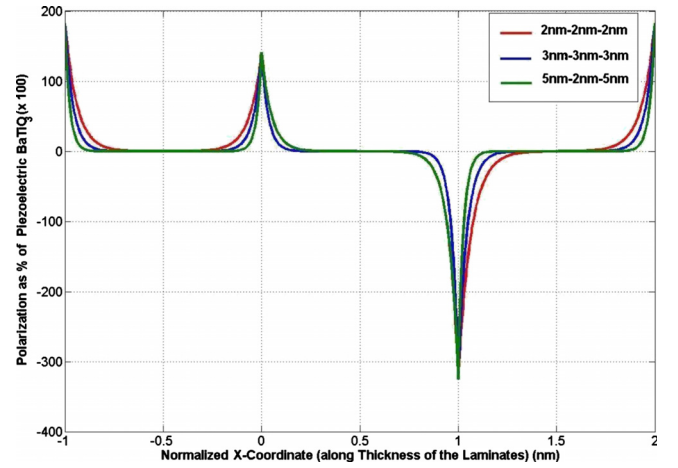
$$P_2 = A_{21} \exp\left(-\frac{x}{l_2}\right) + A_{22} \exp\left(\frac{x}{l_2}\right), \quad (54c)$$

$$u_2 = A_{23} + A_{24}x + \frac{h_2}{c_2} \exp\left(-\frac{x}{l_2}\right) \left[A_{21} + A_{22} \exp\left(2\frac{x}{l_2}\right) \right], \quad (54d)$$

$$P_3 = A_{31} \exp\left(-\frac{x}{l_3}\right) + A_{32} \exp\left(\frac{x}{l_3}\right), \quad (54e)$$

$$u_3 = A_{33} + A_{34}x + \frac{h_3}{c_3} \exp\left(-\frac{x}{l_3}\right) \left[A_{31} + A_{32} \exp\left(2\frac{x}{l_3}\right) \right]. \quad (54f)$$

Boundary conditions are essentially the same as in Sec. IV A. The expressions for polarization in each layer in this case are rather complex (although closed-form), hence only numerical results are presented here (Fig. 9). We consider a “SrTiO₃–MgO–BaTiO₃” three layered superlattice. We take each layer to be 10 nm thick and magnitude of the applied stress to be unity.

FIG. 9. (Color online) Polarization in each layer of a SrTiO₃–MgO–BaTiO₃ periodic three layered superlattice. Overall average polarization in the superlattice is 16% of the piezoelectric BaTiO₃.FIG. 10. (Color online) Polarization in each layer of a SrTiO₃–MgO–BaTiO₃ periodic three layered superlattice for various layer thicknesses.

C. Effect of layer sizes on induced average polarization

Induced average polarization in the periodic three layered superlattice can be fine tuned by controlling the sizes of each layer. We wish to maximize the average polarization in the superlattice with respect to the size of each layer, such that total thickness of the superlattice unit cell does not exceed 20 nm. We restrict the minimum size of each layer to 2 nm. These size-restrictions are based on limitations imposed by current capabilities of state-of-art fabrication processes of ceramic materials. Figure 10 depicts the polarization profiles for various layer thicknesses.

Since the average polarization is inversely proportional to the layer size, we expect that the average polarization will be maximum for smallest possible layer thickness. The solution to this problem in fact confirms this expectation and we obtain a maximum average polarization of 77.5% of piezoelectric BaTiO₃ when each layer is 2 nm thick.

V. CONCLUDING REMARKS

In this paper, we provide exact results for flexoelectric response of thin films under stress and structures based on thin films such as periodic superlattices. The interplay between thin film thickness, symmetry (represented in this context by stacking sequence), and flexoelectricity allows the tantalizing possibility of creating manufacturable apparently piezoelectric thin film superlattices without using piezoelectric materials. In one scenario (trilayer sequence of BTO and MgO with thicknesses in the range of 2 nm), close of 75% of the value of ferroelectric BTO is obtainable.

ACKNOWLEDGMENTS

P.S. and N.D.S. acknowledge financial support from the NSF under NIRT Grant No. CMMI 0708096 and IMI center IIMEC. C.L.M. gratefully acknowledges support from ONR through Contract No. 0014-07-1-0469.

APPENDIX: MATERIAL PROPERTIES

Maranganti and Sharma⁵ recently calculated flexoelectric properties for several dielectrics which agree with the experimental estimates^{13–17,19} to an order of magnitude. However, for the case of BaTiO₃, a large discrepancy with the experimental estimates was observed, reasons for which are still not fully understood. It should be noted that in this current work, we have used the experimental estimates for calculations as shown in the following table:

| | BaTiO ₃ | MgO | SrTiO ₃ |
|---|------------------------|------------------------|------------------------|
| p_{33} (C/N) | 7.80×10^{-11} | ... | 3.00×10^{-14} |
| Lattice parameter (a) (Å) | 4.00 | 4.21 | 3.91 |
| Relative permittivity (–) | 4.00×10^3 | 9.70 | 3.00×10^2 |
| b_{11} (Nm ⁴ /C ²) | 6.77×10^{-06} | 5.67×10^{-08} | 4.14×10^{-06} |
| c_{11} (N/m ²) | 1.62×10^{11} | 3.00×10^{11} | 3.50×10^{11} |
| h_{11} (Nm/C) | -1.55×10^{05} | 1.29×10^{02} | -1.20×10^{03} |
| l_1 (Å) | 1.30 | 1.00 | 1.20 |

¹J. F. Nye, *Physical Properties of Crystals: Their Representation by Tensors and Matrices* (Oxford University Press, New York, 1985), Reprint edition.

²A. Askar, P. C. Y. Lee, and A. S. Cakmak, *Int. J. Solids Struct.* **7**, 523 (1971).

³A. K. Tagantsev, *Phys. Rev. B* **34**, 5883 (1986).

⁴A. K. Tagantsev, *Phase Transitions* **35**, 119 (1991).

⁵R. Maranganti and P. Sharma, *Phys. Rev. B* **80**, 054109 (2009).

⁶T. Dumitrica, C. M. Landis, and B. I. Yakobson, *Chem. Phys. Lett.* **360**, 182 (2002).

⁷S. V. Kalinin and V. Meunier, *Phys. Rev. B* **77**, 033403 (2008).

⁸S. M. Kogan, *Fiz. Tverd. Tela* (Leningrad) **5**, 2829 (1963).

⁹M. Marvan and A. Havránek, *Prog. Colloid Polym. Sci.* **78**, 33 (1988).

¹⁰V. L. Indenbom, V. B. Loginov, and M. A. Osipov, *Kristallografiya* **28**, 1157 (1981).

¹¹M. Marvan and A. Havránek, *Solid State Commun.* **101**, 493 (1997).

¹²W. Ma and L. E. Cross, *Appl. Phys. Lett.* **78**, 2920 (2001).

¹³W. Ma and L. E. Cross, *Appl. Phys. Lett.* **79**, 4420 (2001).

¹⁴W. Ma and L. E. Cross, *Appl. Phys. Lett.* **81**, 3440 (2002).

¹⁵W. Ma and L. E. Cross, *Appl. Phys. Lett.* **82**, 3923 (2003).

¹⁶W. Ma and L. E. Cross, *Appl. Phys. Lett.* **88**, 232902 (2006).

¹⁷J. Y. Fu, W. Zhu, N. Li, and L. E. Cross, *J. Appl. Phys.* **100**, 024112 (2006).

¹⁸W. Ma and L. E. Cross, *Appl. Phys. Lett.* **86**, 072905 (2005).

¹⁹P. Zubko, G. Catalan, A. Buckley, P. R. L. Welche, and J. F. Scott, *Phys. Rev. Lett.* **99**, 167601 (2007).

²⁰G. Catalan, L. J. Sinnamon, and J. M. Gregg, *J. Phys.: Condens. Matter* **16**, 2253 (2004).

²¹J. Fousek, L. E. Cross, and D. B. Litvin, *Mater. Lett.* **39**, 287 (1999).

²²E. A. Eliseev, A. N. Morozovska, M. D. Glinchuk, and R. Blinc, *Phys. Rev. B* **79**, 165433 (2009).

²³R. Maranganti, N. D. Sharma, and P. Sharma, *Phys. Rev. B* **74**, 014110 (2006).

²⁴E. A. Eliseev and A. N. Morozovska, *J. Mater. Sci.* **44**, 5149 (2009).

²⁵N. D. Sharma, R. Maranganti, and P. Sharma, *J. Mech. Phys. Solids* **55**, 2328 (2007).

²⁶L. E. Cross, *J. Mater. Sci.* **41**, 53 (2006).

²⁷M. S. Majdoub, P. Sharma, and T. Cagin, *Phys. Rev. B* **77**, 125424 (2008).

²⁸M. S. Majdoub, P. Sharma, and T. Cagin, *Phys. Rev. B* **78**, 121407(R) (2008).

²⁹M. S. Majdoub and P. Sharma, *Phys. Rev. B* **79**, 115412 (2009).

³⁰J. Yang, *Special Topics in the Theory of Piezoelectricity* (Springer, New York, 2009).

³¹R. D. Mindlin, *Int. J. Solids Struct.* **8**, 369 (1972).

³²R. D. Mindlin, *Int. J. Solids Struct.* **4**, 637 (1968).

³³A. Askar, P. C. Y. Lee, and A. S. Cakmak, *Phys. Rev. B* **1**, 3525 (1970).

³⁴V. S. Maskevich and K. V. Tolpygo, *Sov. Phys. JETP* **5**, 435 (1957).

³⁵R. D. Mindlin, *Int. J. Solids Struct.* **5**, 1197 (1969).

³⁶R. D. Mindlin, *J. Appl. Math. Mech.* **35**, 404 (1971).

³⁷L. D. Landau and E. M. Lifshitz, *Statistical Physics: Course of Theoretical Physics* (Butterworth-Heinemann, London, 1984), Vol. 5.